Biophysical and Molecular Docking Studies of Human Serum Albumin Interactions with a Potential Anticancer Pt(II) Complex

S. Shahraki[a,*], F. Shiri[a] and H. Mansouri-Torshizi[b]

[a]*Department of Chemistry, University of Zabol, Zabol, 05431232186, Iran*
[b]*Department of Chemistry, University of Sistan & Baluchestan, Zahedan, 05433446565, Iran*

ABSTRACT

The interaction between $[Pt(phen)(pyrr\text{-}dtc)]NO_3$ (where phen = 1,10-phenanthroline and pyrr-dtc = pyrrolidinedithiocarbamat) with human serum albumin (HSA) was studied by fluorescence, UV-Vis absorption, circular dichroism (CD) spectroscopy and molecular docking technique under like physiological condition in Tris-HCl buffer solution at pH 7.4. UV-Vis absorption spectroscopy indicates that the protein chain was unfolded upon the addition of Pt(II) complex. Experimental results imply that the Pt(II) complex has a strong ability to quench the intrinsic fluorescence of HSA through a static quenching process. Binding constants (K_b = 2.8, 2.6 and $2.5 \times 10^5 \, M^{-1}$) and the number of binding sites (n ~ 1) were calculated. According to van't Hoff equation, the thermodynamic parameters revealed that hydrophobic forces played a major role when Pt(II) complex interacted with HSA. From the qualitative analysis data of CD spectra, the binding of Pt(II) complex to HSA induced conformational changes in this protein. Finally, a molecular docking was employed for identification of the active site residues and critical interactions involved.

INTRODUCTION

Platinum-based drugs, notably cisplatin, have expanded tremendously for cancer treatment as chemical agents. So far, the major classes of metal-based anticancer drugs include platinum(II) and platinum(IV), palladium(II), gold(I) and gold(III), ruthenium(II) and ruthenium(III), bismuth(III), rhenium(I) and copper(II) compounds, as well as gallium(III) and tin(IV) derivatives, some of them having been reported to demonstrate higher in vitro anticancer activity than cisplatin [1,2]. The importance of platinum-based anticancer agents is reflected by the fact that they are presently used in 50 to 70% of all chemotherapy schemes administered to cancer patients. The key factor explaining why platinum is the most useful element to make active compounds is clearly related to ligand-exchange kinetics. In fact, the chemistry of the platinum coordination compounds is quite different since the Pt-ligand bond, which has the thermodynamic strength of a typical coordination bond, is much weaker than (covalent) C-C and C-N or C-O single and double bonds. However, the ligand-exchange behavior of platinum compounds is quite slow, which gives them a high kinetic stability and results in ligand-exchange reactions of minutes to days, rather than microseconds to seconds for many other coordination compounds [3-5].

Despite the success of cisplatin, it lacks selectivity for tumor tissue, leading to harsh side effects such as renal impairment, nephrotoxicity, neurotoxicity and ototoxicity (loss of balance/hearing), that are only partially reversible when the treatment is stopped. Thus, in order to reduce adverse nephrotoxic effects, sulfur-containing molecules are currently under study as chemo protectants in platinum-based chemotherapy; in particular, dithiocarbamate donors have shown promising properties for clinical use in modulating cisplatin nephrotoxicity [6-9]. The reaction between a primary or secondary amines and carbon disulfide in basic media yields dithiocarbamate ligands. The major benefit of utilizing the small bite-angle of

---

*Corresponding author. E-mail: s-shahraki@uoz.ac.ir;

dithicarbamato moiety as a stabilizing chelating ligand is its unique property to remain intact under a variety of reaction conditions [10].

Human serum albumin (HSA), the most abundant protein in blood plasma, plays an important role in the regulation of plasmatic concentrations of several drugs, including endogenous and exogenous [11,12]. To obtain information on the potential mechanism of the drug–protein interaction, a study of drug action at the molecular level is necessary and HSA is commonly used as a model protein for elucidating drug-protein complexes. Interaction of drug at the protein level will in most cases significantly affect the distribution and elimination rate of drugs *in vivo* [13-15].

In view of the above consideration, the present paper discusses the interaction between a new potential anticancer Pt(II) complex, 1 (Fig. 1) and HSA using different spectral and computational techniques. The results suggest that the hydrophobic interaction played a main role in the binding of complex 1 to HSA. Furthermore, due to complex 1 interaction, changes in protein conformations have also been confirmed from the CD spectra. Finally, molecular docking was applied to provide insight into the interaction of HSA and complex 1.

EXPERIMENTAL

Materials

HSA (fatty acid free, 99%) was purchased from Sigma Aldrich chemical company and used without further purifications. HSA solution was prepared on the basis of its molecular weight of 67,000 Da by dissolving in Tris-HCl buffer (0.1 M, pH 7.4) at the concentration of 5×10^{-5} M and stored at 4 °C. Complex 1 was prepared according to the reported procedure [17]. Accurate protein concentration was determined spectrophotometrically using an extinction coefficient of 35219 M^{-1} cm^{-1} at 280 nm [18]. Stock solution of the complex (5×10^{-4} M) was prepared by dissolving the complex in doubly distilled water. NaCl (analytical grade, 1 M) solution was used to maintain the ionic strength of buffer at 0.1 M; pH was adjusted to 7.4 by using HCl. Working standard solution was obtained by appropriate dilution of the stock solution. All other reagents were of analytical grade and ultra-pure water was used throughout all the experiments.
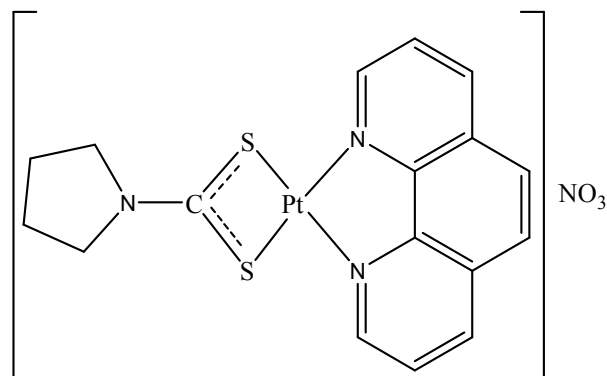
Fig. 1. Molecular structure of [Pt(phen)(pyrr-dtc)]NO$_3$.

Spectroscopic Studies

UV-Vis spectra of complex 1 and HSA solutions were recorded on a J$_{ASCO}$ UV-Vis-7850 recording spectrophotometer in the range of 200-400 nm. The HSA-binding and denaturation experiments were performed separately at three temperatures 292, 302 and 312 K in Tris-HCl buffer medium. Intrinsic fluorescence measurements of HSA in the presence of complex 1 were performed on a Varian spectrofluorimeter model Cary Eclipse with 1.0 cm quartz cells, the widths of both the excitation and emission slit were set as 5 nm. The excitation wavelength was set at 280 nm to selectively excite the tryptophan and tyrosine residues, and the emission spectra were recorded between 300 and 500 nm with maximum observed at 350 nm. The experiments were performed at several [drug]/[protein] molar ratios. CD spectra were measured on a J-810 with a 1 mm path length at room temperature.

Molecular Docking

Molecular docking was carried out using smina [19] which uses the AutoDock Vina [20] scoring function by default. The 3D X-ray structure of human serum albumin was taken from the protein data bank (PDB) encoded 1O9X. The structure of complex 1 files were provided using AutoDock Tools. After that, energy minimization calculations were carried out with Density Functional Theory (DFT) procedure in B3LYP level and fundamental set for Pt and all other atoms adapt to LanL2DZ and 6-31G respectively, using Gaussian 09. For the recognition of the

binding sites in HSA, blind docking was carried out with setting of grid size to 88, 68 and 72 along x, y, and z axes with a grid spacing of 1 Å after assigning the protein and probe with Kollman charges. The grid center was set at 20, 70, and 10 Å. All other parameters were default settings. Smina was run with default settings, which samples nine complex 1 conformations using the Vina docking routine of Monte Carlo stochastic sampling. The lowest energy docked conformation, according to the smina scoring function, was selected as the binding mode. The output from smina was presented with BIOVIA Discovery Studio client 2016 [21]. The interacting energies between each amino acid with the best pose of docked ligand and complex into HSA binding site were calculated by Molegro Molecular Viewer 2.5 (MMV) (http:// www.molegro.com/mmv-product.php).

RESULTS AND DISCUSSION

UV-Vis Absorption Spectral Measurements

We measured the UV-Vis absorbance spectra of HSA (6 μM) when this protein was exposed to various amounts of complex 1 (0 to 160 μM) (Fig. 2). Also the absorbance at λ_{max} = 280 nm was monitored for either HSA or mixtures of HSA with Pt(II) complex (Fig. 3). These experiments were carried out separately at three temperatures of 292, 302 and 312 K in Tris-HCl buffer medium. Addition of metal complex to HSA solution continued until no further changes in the absorption readings were observed. As can be seen in Fig. 2 and Fig. 3, the absorbance of HSA is increased regularly with increasing the concentration of the complex 1. This indicates that the polypeptide chain of HSA successively unfolded upon the addition of this complex. The concentration of metal complex in the midpoint of transition, $[L]_{1/2}$, at 292, 302 and 312 K was obtained 89, 84 and 75 μM respectively. These values revealed that an increase in the temperature accompanies the lower stability of the HSA toward denaturation which can be attributed to the presence of the complex 1.

### Fluorescence Quenching of HSA by Complex 1

Fluorescence quenching of the tryptophan residues in HSA was also monitored to measure the drug-binding affinity. The addition of drug to HSA solution caused a decrease in intrinsic fluorescence emission spectra of the protein upon excitation at 295 nm. Figure 4 shows the fluorescence emission spectra of HSA in the presence of different concentration of complex 1 at physiological condition (pH 7.4). The emission spectrum of HSA is characterized by a broad emission band at 350 nm. As it could be seen in Fig. 4 the fluorescence intensity of HSA decreased gradually with the increase of complex 1 concentration. However, the maximum emission wavelength of HSA barely changed during the interaction, suggesting that Trp residues did not expose to any change in polarity, and the interaction may occur via the hydrophobic region located inside HSA [22].

Fluorescence quenching occurs by different mechanisms, usually classified as dynamic quenching and static quenching. Dynamic and static quenching can be distinguished by their different dependences on temperature. Because higher temperatures result in larger diffusion coefficients, the quenching constants are expected to increase with a gradually increasing temperature in dynamic quenching. Although the increase of temperature is likely to result in a smaller static quenching constant due to the dissociation of weakly bound complexes [23]. Commonly, Fluorescence quenching can be described by the following Stern-Volmer equation:

$$\frac{F_0}{F} = 1 + K_q \tau_0 [Q] = 1 + K_{sv}[Q]$$

where F_0 and F are the fluorescence intensities before and after the addition of the quencher (complex 1), respectively, K_{sv} is the Stern-Volmer quenching constant, kq is the bimolecular quenching constant, τ_0 is the lifetime of the fluorophore in the absence of the quencher (10^{-8} s), and [Q] is the concentration of the quencher. Stern-Volmer plots of the HSA fluorescence quenching by complex 1 are given in Fig. 5, and the calculated K_{sv} and kq values are summarized in Table 1. Here the values of kq are much greater than the maximum diffusion collision quenching rate constant of various quenchers with the biopolymer [23]. This suggests that the quenching of Trp fluorescence occurred via a specific interaction between HSA and complex 1, and static quenching is the dominant mechanism [24]. Moreover, K_{sv} is inversely correlated with temperature, which indicates
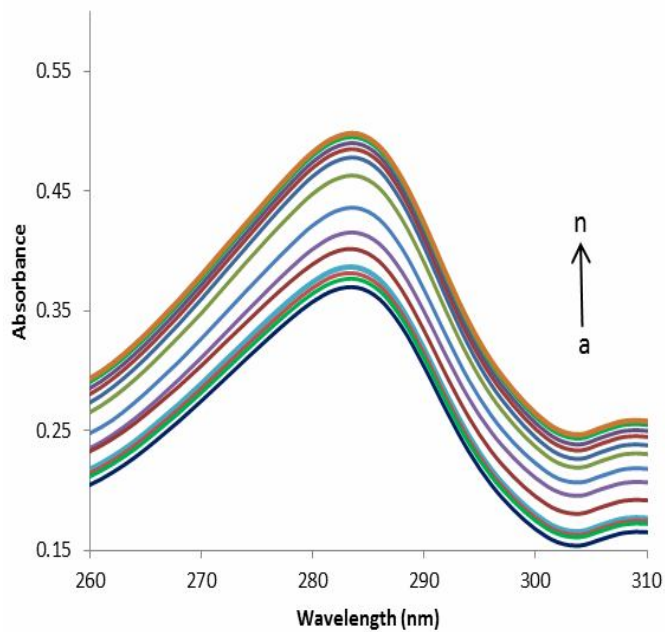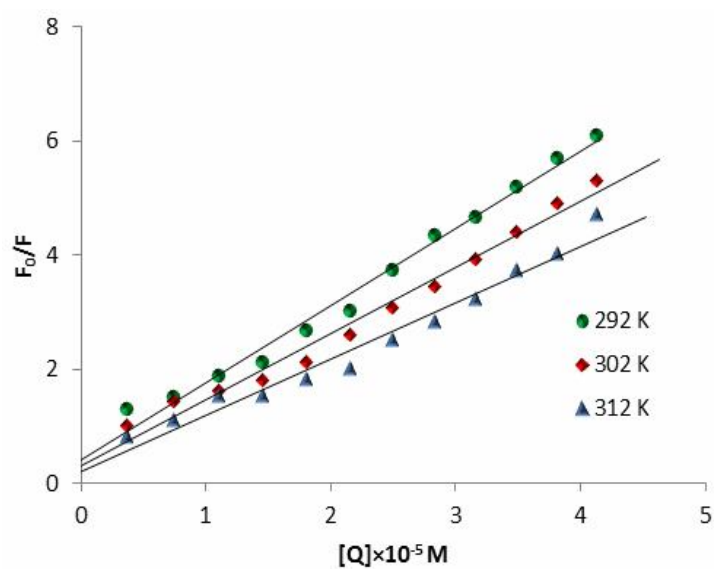
Fig. 2. Absorption spectra of HSA (6 µM)) (1), with various amounts of Pt(II) complex (0-160 µM) at 302 K.
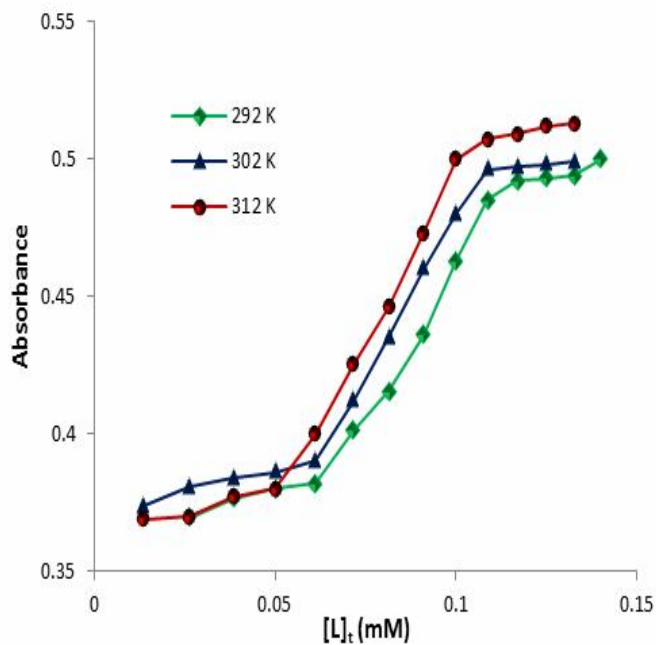
Fig. 3. The changes of absorbance of HSA at λ_{max} = 280 nm due to increasing the total concentration of [Pt(phen)(pyrr-dtc)NO$_3$,[L]t, at constant temperature of 292, 302 and 312 K.
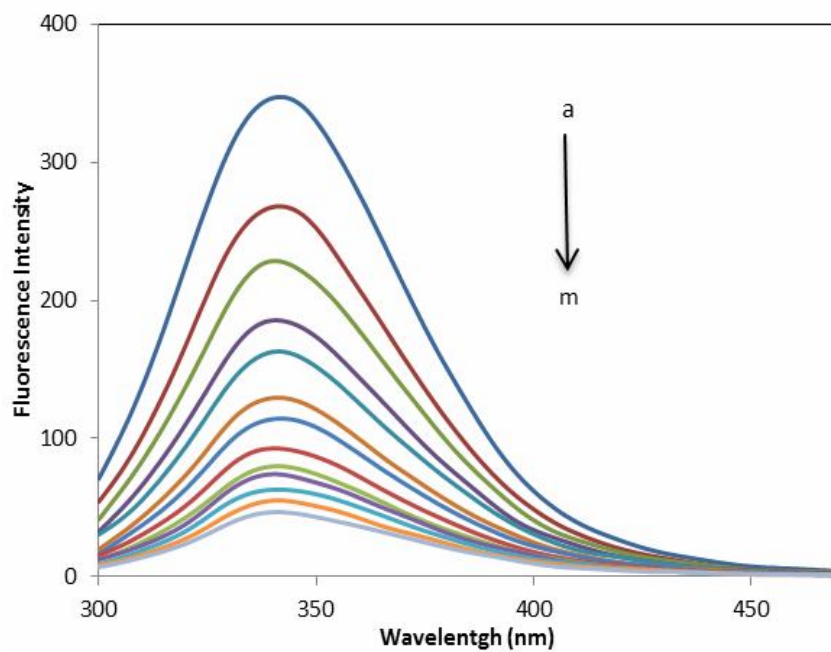
Fig. 4. Effect of Pt(II) complex on the fluorescence spectrum of HSA at 312 K, [HSA] = 6 μM, [complex 1] [1-13] = 5-90 μM

Fig. 5. Stern-Volmer plots for the interaction of Pt(II) complex and HSA at different temperatures.

Table 1. Sertern-Volmer Quenching Constants for the Interaction of Pt(II) Complex with HSA

T (K)	K_{sv} (10^5 M^{-1})	kq (10^{13} $M^{-1}s^{-1}$)	SD[a]	R[b]
292	1.15	1.15	0.0011	0.9877
302	1.01	1.01	0.0036	0.9828
312	0.82	0.82	0.0102	0.9670

[a]SD is the standard deviation of three measurements. [b]R is the correlation coefficient.

Table 2. Binding and Thermodynamic Parameters of HSA Interaction with Pt(II) Complex

T (K)	K_b (10^4 M^{-1})	SD[a]	N	ΔG (kJ mol^{-1})	ΔH (kJ mol^{-1})	ΔS (J mol^{-1} K^{-1})
292	28.195	0.0321	1.42	- 70.09		
302	26.334	0.0056	1.39	- 70.95	- 44.92	86.21
312	25.910	0.0112	1.42	- 71.82		

[a]SD is the standard deviation of three measurements.
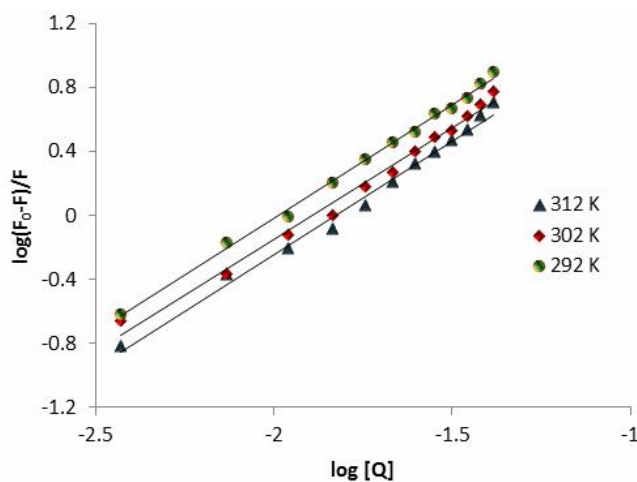

Fig. 6. Plots of log(F_0 - F)/F against log[complex] for Pt(II) complex quenching effect on HSA fluorescence at different temperatures

that the fluorescence quenching of HSA by complex 1**,** is not a dynamic process but a static process.

Binding Constant and Number of Binding Sites

For static quenching, the relationship between fluorescence quenching intensity and the concentration of quenchers can be described by the binding constant formula [25,26]:

$$M + nQ = MQ_n$$
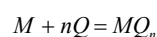
$$\log\frac{(F_0 - F)}{F} = \log K_b + n\log[Q]$$

Where Q is the quencher, M is the bio macromolecule with fluorophores, MQ_n is binary complex, whose binding constant and number of binding sites is K_b and n respectively, F_0 and F represent the fluorescence intensities in the absence and in the presence of quencher. A plot of log $(F_0 - F)/F$ *vs*. log[Q] will give a straight line with a slope of n and y-axis intercept of $\log K_b$ (Fig. 6). The corresponding results at 292, 302 and 312 K are shown in Table 1. The values of n approximate to 1, suggesting that only one reactive site exists in HSA for complex 1, and the binding constants decreased with increasing temperature, which coincided with the Stern-Volmer quenching constants.

Thermodynamic Parameters and the Nature of Binding Forces

Considering the dependence of binding constant on temperature, a thermodynamic process was considered to be responsible for the formation of a complex. Therefore, the thermodynamic parameters dependent on temperatures were analyzed in order to further characterize the acting forces between complex 1 and HSA. The acting forces between a small molecule and macromolecule mainly include hydrogen bonds, van der Waals forces, electrostatic forces and hydrophobic interaction forces. The thermodynamic parameters, enthalpy change (ΔH), entropy change (ΔS) and free energy change (ΔG) are the main evidences to determine the binding mode. From the viewpoint of thermodynamics, $\Delta H > 0$ and $\Delta S > 0$ imply a hydrophobic interaction; $\Delta H < 0$ and $\Delta S < 0$ reflect the van der Waals force or hydrogen bond; $\Delta H < 0$ and $\Delta S > 0$ suggest an electrostatic force [27]. The thermodynamic parameters were evaluated using the following equations:

$$\ln K = -\frac{\Delta H}{RT} + \frac{\Delta S}{R}$$

$$\Delta G = \Delta H - T\Delta S$$

where K and R are the binding constant and gas constant, respectively. From the linear relationship between LnK and the reciprocal absolute temperature 1/T (Fig. 7), the ΔH and ΔS values were determined and the corresponding values of

ΔG are also calculated from Eq. (7). The results obtained are shown in Table 2.

The negative values of free energy (ΔG) supported the assertion that the binding process was spontaneous. The negative ΔH value (-44.92 kJ mol^{-1}) observed cannot be mainly attributed to electrostatic interactions, since for electrostatic interactions, ΔH is very small, almost zero [28]. From these results, therefore, the binding of complex 1 to HSA appears to involve hydrophobic interactions as shown by the positive value of ΔS although a lower component of electrostatic interactions cannot be excluded [29-31].

## Fluorescence Resonance Energy Transfer between HSA and Complex 1

Fluorescence resonance energy transfer (FRET) is a distance-dependent interaction between the different electronic excited states of dye molecules in which excitation energy is transferred from one molecule (donor) to another molecule (acceptor) at the cost of the emission from the former molecular system [32]. Generally FRET occurs whenever the emission spectrum of donor (here tryptophan residue of the HSA) overlaps with the absorption spectrum of acceptor (here complex 1). The overlap of the UV-Vis absorption spectrum of complex 1 with the fluorescence emission spectrum of HSA is shown in Fig. 8. The distance between the donor and acceptor can be calculated according to Foster's theory. The energy transfer efficiency E and the distance between the acceptor and donor r can be defined as the following equations [33-35]:

$$E = 1 - \frac{F}{F_0} = \frac{R_0^6}{R_6^0 + r_0^6}$$

where F and F_o are the fluorescence intensities of HSA in the presence and absence of complex 1 and R_o is the critical distance when the transfer efficiency is 50%. The value of R_o was calculated using the equation:

$$R_0^6 = 8.8 \times 10^{-25} K^2 N^{-4} \Phi J$$

where K^2 is spatial orientation factor of the dipole, N is refractive index of the medium, Φ is fluorescence quantum yield of the donor and J is overlap integral of the
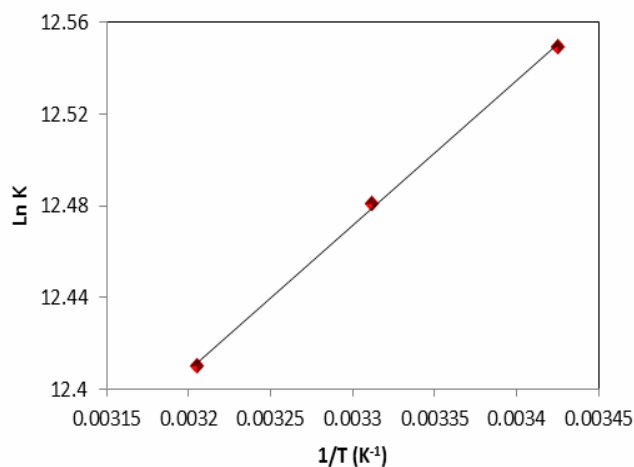
Fig. 7. Arrhenius plots for the interaction of Pt(II) complex and HSA at different temperatures.
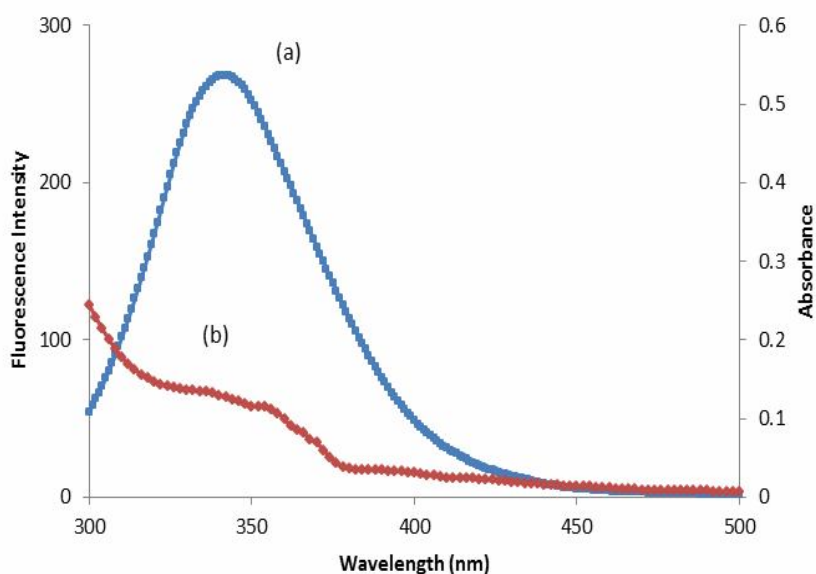
Fig. 8. Spectral overlap between the absorption spectrum of Pt(II) complex (6 μM) (a) and fluorescence emission spectrum of HSA (6 μM) (b) at 312 K.

fluorescence emission spectrum of donor and absorption spectrum of the acceptor and calculated by the following equation:

$$J = \frac{\Sigma F(\lambda)\varepsilon(\lambda)\lambda^4 \Delta\lambda}{\Sigma F(\lambda)\Delta\lambda}$$

where $F(\lambda)$ is the corrected fluorescence intensity of the donor at wavelength λ and $\varepsilon(\lambda)$ is the molar absorption coefficient of the acceptor at wavelength λ. In the present case, $K^2 = 2/3$, $n = 1.336$ and $\Phi = 0.15$ [36]. The J, R_0, E and r were calculated and shown in Table 3. The r value is in the range of 2-8 nm, which means that it is possible that

Table 3. The Calculated Values of Overlap Integral and Forster Distance for HSA-Pt(II) Complex Energy Transfer

J (cm^3 l mol^{-1})	E	R_0 (nm)	r (nm)
1.51×10^{-15}	0.088	4.56	4.61

Table 4. The conformational Changes of HSA in the Absence and Presence of Pt Complex

	α-helix	Antiparallel	Parallel	β-Turn	Random-coil
HSA	51.73 %	3.55%	4.11%	12.19%	28.40%
HSA + Pt complex (1:1)	48.03%	4.12%	4.75%	14.01%	29.10%
HSA + Pt complex (1:10)	36.76%	4.98%	5.13%	15.31%	37.83%

Table 5. Smina Score of HSA with Different Conformers of Complex 1

Pose	Affinity (kcal mol^{-1})
1	-8.4
2	-8.1
3	-8.1
4	-7.7
5	-7.6
6	-7.4
7	-7.3
8	-7.2
9	-7.2

the energy transfer can take place between complex 1 and HSA. Also, the larger value of r compared to that of R_0 revealed the presence of static type of quenching mechanism [37].

Circular Dichroism Spectra

Circular dichroism (CD) spectroscopy is a very basic and sensitive technique to monitor the secondary structural change of protein upon the interactions with ligands. The CD spectra of HSA exhibit two negative bands in the far ultraviolet region at 208 and 220 nm, which represent the transition of π→π* and n→π* of α-helix structure of protein [38]. Figure 9 shows the CD spectra of HSA in the absence and presence of complex 1. It can be observed that with the increase in complex 1 concentration, the CD signal of HSA increased, suggesting that the binding of complex 1 to HSA induces a significant conformational change in HSA. However, the CD spectra of HSA in the presence or absence of complex 1 are similar in shape, indicating that the structure of HSA is also predominantly α-helical. The fractions of α-Helix, Parallel, β-Turn and Random Coil structures are listed in Table 4. The results showed a
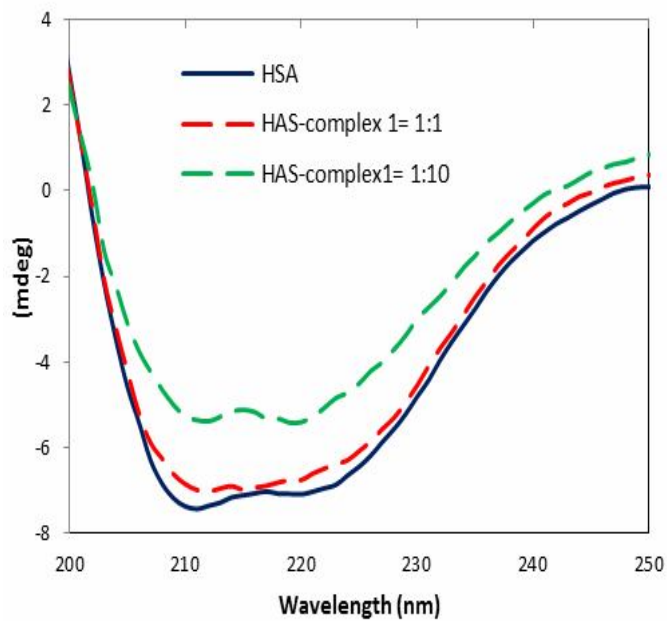
Fig. 9. CD spectra of the free HSA (5 μM) and HSA in presence of 5 and 50 μM Pt(II) complex.
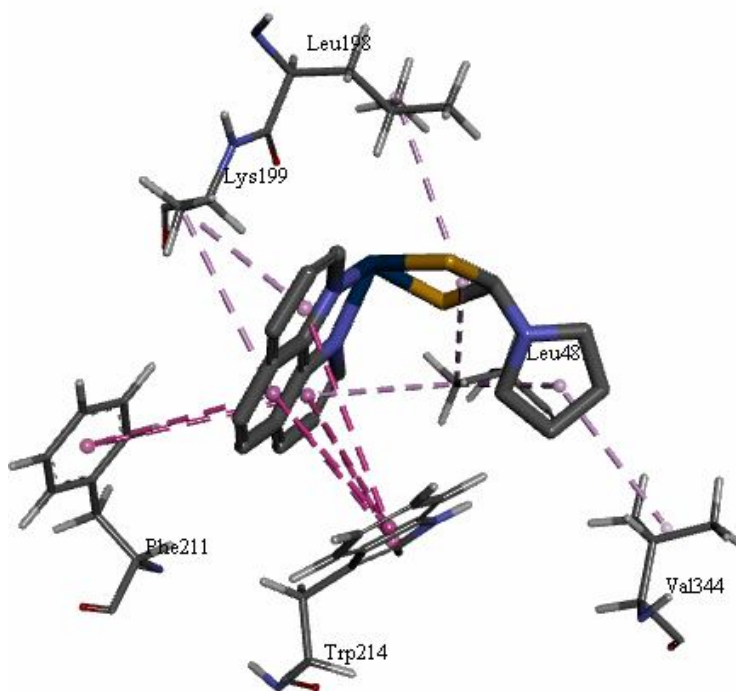
Fig. 10. The best docked conformation of complex 1 in the in the binding site of HSA from Smina.
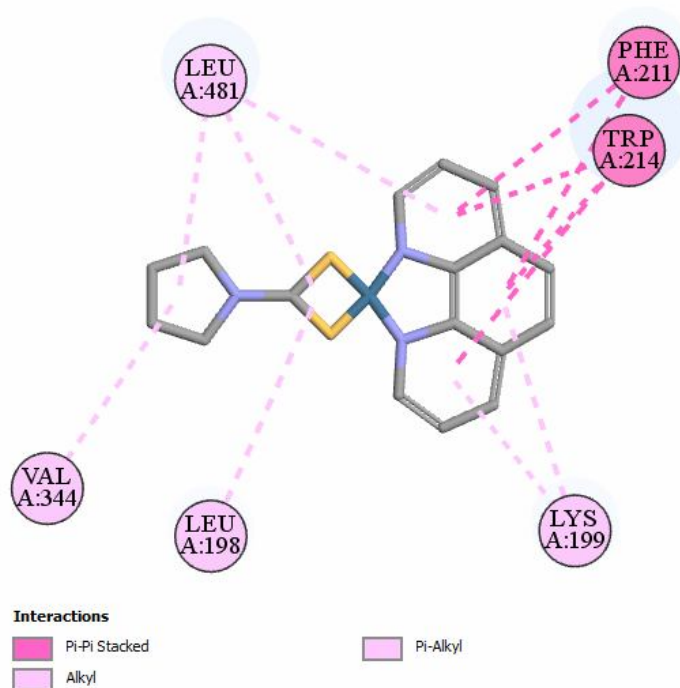
Fig. 11. Two-dimensional scheme of interactions between the Complex 1 and HSA. Only the more important residues for binding are shown.

Table 6. Interaction Energy between the Pt Complex and Responsive Amino Acid Residues in Molecular Docking

Amino acid residues	Interaction energy (kJ mol^{-1})
Ala210	-1.764
Glu450	-5.251
His242	-0.332
Leu198	-7.807
Leu481	-8.673
Lys195	-2.211
Lys199	-11.026
Phe206	-0.377
Phe211	-11.974
Ser202	-9.271
Ser454	-4.422
Trp214	-31.379
Val344	-4.179

decrease in α-helix content and an increase in the β-sheet and Random Coil formation which reveals that the interaction between complex 1 and HSA leads to a change of secondary structure of the protein [39,40].

Molecular Docking Analysis

In silico modeling approaches such as molecular docking [16] are effective tools for predicting putative binding sites and binding affinities. Molecular docking computations were carried out to give insight about binding conformations of the complex 1 with the active site of the HSA. HSA consists of 585 amino acid residues organized in three domains (I, II, III), each comprising two subdomains (A, B). The main binding sites on HSA are located in hydrophobic cavities in subdomains IIA and IIIA, such as tryptophan (Trp214) and tyrosine (Tyr411) residues. Allowing to smina output, 9 conformations for complex 1 were achieved; the energy binding of all conformations are shown in Table 5. The best docked conformation of the complex 1 was associated to binding energy -8.4 kcal mol^{-1} and is shown in Fig. 10 with the labeled key residues. 2D schematic interaction model of complex 1 (Fig. 11) was used to investigate and clarify the interactions between complex 1 and receptor. Furthermore, the interaction energy between the complex 1 and amino acid residues are listed in Table 6. Detailed analysis of the binding mode of the best docked pose of complex 1 shows that some pi-alkyl and alkyl interactions between the Leu481, Val344, Leu198, Lys199 and complex 1. As it can be seen in Fig. 10, Trp214 was located beside the complex 1 and it can be highly relevant to the highest energy interaction with HSA (-31.379 kJ mol^{-1}); consequently, the energy transferred from the excited Trp214 residue to complex 1, induces the quenching of the fluorescence emission of HSA.

CONCLUSIONS

In the present work, the binding of [Pt(phen)(pyrr-dtc)]NO$_3$ to HSA were investigated by using UV-Vis absorption, fluorescence and circular dichroism spectroscopy and then confirmed by molecular docking study. UV-Vis and CD spectra revealed that the conformational and micro environmental changes in HSA structure *via* the binding of complex 1. The results of fluorescence spectroscopy indicated that the probable quenching mechanism of fluorescence of HSA by complex 1 was a static quenching procedure. The thermodynamic parameters indicated that hydrophobic interaction played major role during the interaction. Various binding parameters have been evaluated and discussed. The docking results are in good agreement with the experimental results obtained by multi-spectroscopic methods. We hope that such spectroscopic and docking studies to be indeed helpful in studying the pharmacological response of drugs and design of dosage forms.

ACKNOWLEDGEMENTS

REFERENCES

[1] T. Connors, M. Jones, W. Ross, P.D. Braddock, A. Khokhar, M. Tobe, Chem. Biol. Interact. 5 (1972) 415.

[2] M. Frezza, S. Hindo, D. Chen, A. Davenport, S. Schmitt, D. Tomco, Q. Ping Dou, Curr. Pharm. Des. 16 (2010) 1813.

[3] J. Reedijk, Proc. Natl. Acad. Sci. U.S.A., 100 (2003) 3611.

[4] A.S. Abu-Surrah, M. Kettunen, Curr. Med. Chem. 13 (2006) 1337.

[5] J. Reedijk, Platinum Met. Rev. 52 (2008) 2.

[6] A.M. Florea, D. Büsselberg, Cancers 3 (2011) 1351.

[7] V. Alverdi, L. Giovagnini, C. Marzano, R. Seraglia, F. Bettio, S. Sitran, R. Graziani, D. Fregona, J. Inorg. Biochem. 98 (2004) 1117.

[8] C. Marzano, L. Ronconi, F. Chiara, M.C. Giron, I. Faustinelli, P. Cristofori, A. Trevisan, D. Fregona, Int. J. Cancer. 129 (2011) 487.

[9] G. Faraglia, D. Fregona, S. Sitran, L. Giovagnini, C. Marzano, F. Baccichetti, U. Casellato, R. Graziani, J. Inorg. Biochem. 83 (2001) 31.

[10] S. Shahraki, H. Mansouri-Torshizi, A. Heydari, A. Ghahghaei, A. Divsalar, A. Saboury, H. Ghaemi, M. Doostkami, S. Zareian, Iran. J. Sci. Technol. 39 (2015) 187.

[11] W.H. Ang, E. Daldini, L. Juillerat-Jeanneret, P.J. Dyson, Inorg. Chem. 46 (2007) 9048.

[12] P. Lee, X. Wu, Curr. Pharm. Des. 21 (2015) 1862.

[13] G. Lupidi, A. Scire, E. Camaioni, K. Khalife, G. De Sanctis, F. Tanfani, E. Damiani, Phytomedicine 17 (2010) 714.

[14] F. Yang, Y. Zhang, H. Liang, Int. J. Mol. Sci. 15 (2014) 3580.

[15] A. Virkamäki, K. Ueki, C.R. Kahn, J. Clin. Invest. 103 (1999) 931.

[16] D.A. Gschwend, A.C. Good, I.D. Kuntz, J. Mol. Recognit., 91 (1996) 175.

[17] H. Mansouri-Torshizi, S. Shahraki, Z.S. Nezami, A. Ghahghaei, S. Najmedini, A. Divsalar, H. Ghaemi, A.A. Saboury, Complex Met. 1 (2014) 23.

[18] C.N. Pace, F. Vajdos, L. Fee, G. Grimsley, T. Gray, Protein Sci. 4 (1995) 2411.

[19] D.R. Koes, M.P. Baumgartner, C.J. Camacho, J. Chem. Inf. Model 53 (2013) 1893.

[20] O. Trott, A. J. Olson, J. Comput. Chem. 31 (2010) 455.

[21] A.D.S. Client, Calif, USA Accelrys.

[22] J.R. Lakowicz, C.D. Geddes, Topics in Fluorescence Spectroscopy. 1991, Springer.

[23] B.T. Yin, C.Y. Yan, X.M. Peng, S.L. Zhang, S. Rasheed, R.X. Geng, C.H. Zhou, Eur. J. Med. Chem. 71 (2014) 148.

[24] Y.J. Hu, Y. Liu, X.H. Xiao, Biomacromolecules 10 (2009) 517.

[25] X. Song, G. Huhle, L. Wang, J. Harenberg, Thromb. Res. 99 (2000) 195.

[26] Y. Zhang, M. Wang, Q. Xie, X. Wen, S. Yao, Sensor. Actuat. B-Chem. 105 (2005) 454.

[27] P. Qu, H. Lu, X. Ding, Y. Tao, Z. Lu, J. Mol. Struct. 920 (2009) 172.

[28] P. Kandagal, S. Ashoka, J. Seetharamappa, S. Shaikh, Y. Jadegoud, O. Ijare, J. Pharm. Biomed. Anal. 41 (2006) 393.

[29] Q. Wang, J. Yan, J. He, K. Bai, H. Li, J. Lumin. 138 (2013) 1.

[30] Q. Bian, J. Liu, J. Tian, Z. Hu, Int. J. Biol. Macromol. 34 (2004) 275.

[31] G. Dehghan, M. Shaghaghi, S. Sattari, A. Jouyban, J. Lumin. 149 (2014) 251.

[32] J. Abraham, B. Mathew, Synergic Effects of Anticancer Drugs to Bovine Serum Albumin: A Spectroscopic Investigation. Research Journal of Recent Sciences, ISSN, 2277, 2502.

[33] J. Tian, J. Liu, X. Tian, Z. Hu, X. Chen, J. Mol. Struct. 691 (2004) 197.

[34] F. Wang, W. Huang, Z. Dai, J. Mol. Struct. 875 (2008) 509.

[35] Y.J. Hu, Y. Liu, W. Jiang, R.M. Zhao, S.S. Qu, Photobiol. B, Biol. 80 (2005) 235.

[36] D.E. Epps, T.J. Raub, V. Caiolfa, A. Chiari, M. Zamai, J. Pharm. Pharmacol. 51 (1999) 41.

[37] W. He, Y. Li, C. Xue, Z. Hu, X. Chen, F. Sheng, Bioorg. Med. Chem. 13 (2005) 1837.

[38] L. Trynda-Lemiesz, A. Karaczyn, B.K. Keppler, H. Kozlowski, J. Inorg. Biochem. 78 (2000) 341.

[39] Z. Lu, T. Cui, Q. Shi, Applications of Circular Dichroism and Optical Rotatory Dispersion in Molecular Biology. Science, Beijing, 1987, pp. 79-82.

[40] F.L. Cui, J. Fan, J.P. Li, Z.D. Hu, Bioorgan. Med. Chem. 12 (2004) 151.